Outer-membrane lipoprotein LpoB spans the periplasm to stimulate the peptidoglycan synthase PBP1B

Alexander J. F. Egan[a,1], Nicolas L. Jean[b,c,d,1], Alexandra Koumoutsi[e,1], Catherine M. Bougault[b,c,d], Jacob Biboy[a], Jad Sassine[a], Alexandra S. Solovyova[f], Eefjan Breukink[g], Athanasios Typas[e,2], Waldemar Vollmer[a,2], and Jean-Pierre Simorre[b,c,d,2]

[a]Centre for Bacterial Cell Biology, [f]Institute for Cell and Molecular Biosciences, Newcastle University, Newcastle upon Tyne NE2 4AX, United Kingdom; [b]Institut de Biologie Structurale, Université Grenoble Alpes, F-38027 Grenoble, France; [c]Institut de Biologie Structurale, Direction des Sciences du Vivant, Commissariat à l'Energie Atomique, F-38027 Grenoble, France; [d]Institut de Biologie Structurale, Centre National de la Recherche Scientifique, F-38027 Grenoble, France; [e]European Molecular Biology Laboratory, Genome Biology Unit, 69117 Heidelberg, Germany; and [g]Department of Biochemistry of Membranes, Bijvoet Center for Biomolecular Research, University of Utrecht, 3584 CH, Utrecht, The Netherlands

Edited by Caroline S. Harwood, University of Washington, Seattle, WA, and approved April 14, 2014 (received for review January 8, 2014)

Bacteria surround their cytoplasmic membrane with an essential, stress-bearing peptidoglycan (PG) layer. Growing and dividing cells expand their PG layer by using membrane-anchored PG synthases, which are guided by dynamic cytoskeletal elements. In *Escherichia coli*, growth of the mainly single-layered PG is also regulated by outer membrane-anchored lipoproteins. The lipoprotein LpoB is required for the activation of penicillin-binding protein (PBP) 1B, which is a major, bifunctional PG synthase with glycan chain polymerizing (glycosyltransferase) and peptide cross-linking (transpeptidase) activities. Here, we report the structure of LpoB, determined by NMR spectroscopy, showing an N-terminal, 54-aa–long flexible stretch followed by a globular domain with similarity to the N-terminal domain of the prevalent periplasmic protein TolB. We have identified the interaction interface between the globular domain of LpoB and the noncatalytic UvrB domain 2 homolog domain of PBP1B and modeled the complex. Amino acid exchanges within this interface weaken the PBP1B–LpoB interaction, decrease the PBP1B stimulation in vitro, and impair its function in vivo. On the contrary, the N-terminal flexible stretch of LpoB is required to stimulate PBP1B in vivo, but is dispensable in vitro. This supports a model in which LpoB spans the periplasm to interact with PBP1B and stimulate PG synthesis.

Peptidoglycan (PG) is an essential component of the bacterial cell envelope, required for cell shape and stability. It is composed of glycan chains that are connected by short peptides, and forms a net-like, elastic structure, called the sacculus, which encases the cytoplasmic/inner membrane (IM) (1). In Gram-negative bacteria, such as *Escherichia coli*, the sacculus is mainly single-layered and is firmly attached to the outer membrane (OM) by abundant OM proteins. Some of the most effective antibiotic agents, such as the β-lactams and glycopeptides, inhibit PG biosynthesis, resulting in cell lysis.

Bacteria enlarge their sacculus by polymerizing new PG from lipid II precursor at the outer face of the IM and incorporating the newly made material into the existing PG layer. At the same time, a significant amount of old material is released. For synthesis and hydrolysis to be coupled, the corresponding enzymes have to be tightly regulated and coordinate their actions (2). How does this happen? The current view is that PG synthases [penicillin-binding proteins (PBPs)] and hydrolases form membrane-anchored multienzyme complexes, which are driven by cytoskeletal elements. More recently, it was established that dedicated regulators tightly control the activities of PG synthases and hydrolases and/or couple it to other cell envelope processes (3–6).

PG synthesis requires glycosyltransferases (GTases) to polymerize the glycan chains and transpeptidases (TPases) to form peptide cross-links. Most bacteria carry several PG synthases, which can perform one or both enzymatic reactions. In *E. coli*, the bifunctional GTase/TPases PBP1A and PBP1B provide the main PG synthesis activity, and the cell needs one of them to survive. *E. coli* has also two monofunctional TPases, PBP2 and PBP3, which have essential roles in cell elongation and division, respectively. Recent localization and biochemical data suggest that PBP1A works mainly together with PBP2 during cell elongation (7), when PG synthesis is guided by the actin-like MreB. On the contrary, PBP1B and PBP3 interact with each other, as well as with other essential cell division proteins, such as FtsW and FtsN (8–10), and they colocalize at the division site. They are both part of the divisome, a large protein complex, which is nucleated by the tubulin-like FtsZ during cell division to synthesize and split the cell envelope layers, including the PG, and produce new cell poles (11).

Recent work showed that, in *E. coli*, and presumably other Gram-negative bacteria, PG synthesis is also regulated from outside the sacculus by OM-anchored lipoproteins. LpoA and LpoB interact with their cognate PG synthase, PBP1A and PBP1B, respectively, and stimulate their activity, which is essential for the function of the PBPs in vivo (3, 5). This suggests that the OM-anchored Lpo proteins have to penetrate the elastic sacculus net before reaching their cognate, cytoplasmic

Significance

Bacteria surround their cytoplasmic membrane with an essential heteropolymer, the peptidoglycan (PG) sacculus, to maintain osmotic stability and cell shape. Cells enlarge their sacculus by using cytoplasmic membrane-anchored PG synthases, which are guided by cytoskeletal elements. Gram-negative bacteria have a thin, mainly single-layered sacculus, connected to the outer membrane. Outer-membrane–anchored lipoproteins were recently found to be essential for PG growth. Here, we present the structure of the outer membrane protein LpoB of *Escherichia coli*, which is required for the function of the major PG synthase PBP1B. LpoB has a long, flexible N-terminal stretch enabling it to span the periplasm and reach its docking site in PBP1B, the noncatalytic UvrB domain 2 homolog domain, to stimulate PG growth.

Author contributions: A.J.F.E., N.L.J., A.K., C.M.B., A.S.S., A.T., W.V., and J.-P.S. designed research; A.J.F.E., N.L.J., A.K., C.M.B., J.B., J.S., A.S.S., A.T., and J.-P.S. performed research; E.B. contributed new reagents/analytic tools; A.J.F.E., N.L.J., A.K., C.M.B., J.B., A.S.S., A.T., W.V., and J.-P.S. analyzed data; and A.J.F.E., N.L.J., A.K., C.M.B., A.S.S., A.T., W.V., and J.-P.S. wrote the paper.

The authors declare no conflict of interest.

This article is a PNAS Direct Submission.

Freely available online through the PNAS open access option.

Data deposition: The atomic coordinates have been deposited in the Protein Data Bank, www.pdb.org (PDB ID code 2MII). The NMR chemical shifts have been deposited in the BioMagResBank, www.bmrb.wisc.edu (accession no. 19681).

[1]A.J.F.E., N.L.J., and A.K. contributed equally to this work.

[2]To whom correspondence may be addressed. E-mail: typas@embl.de, w.vollmer@ncl.ac.uk, or jean-pierre.simorre@ibs.fr.

This article contains supporting information online at www.pnas.org/lookup/suppl/doi:10.1073/pnas.1400376111/-/DCSupplemental.

membrane-anchored PBP. We have postulated that this allows the cell to control the rate of PG synthesis in response to the local pore size of the sacculus. This hypothesis couples PG growth with overall cell growth, allowing for PG synthesis to rapidly adjust to environmental cues (2, 5).

The crystal structure of PBP1B has been determined (12). In addition to the GTase and TPase domains, PBP1B harbors a small, noncatalytic UvrB domain 2 homolog (UB2H) domain (Pfam 14814), which is unique to this synthase. Based mostly on genetic evidence, we previously suggested that the UB2H domain acts as a docking domain for LpoB (5). In this work, we have determined the structure of a soluble version of LpoB by NMR spectroscopy. LpoB has a 54-aa–long unstructured and flexible stretch at its N terminus, followed by a globular domain, which interacts with the purified UB2H domain. We have mapped the interface between the two proteins by NMR spectroscopy, providing, to our knowledge, the first structural characterization of an interaction between a PG-related enzyme and its regulator. Targeted substitutions in amino acids within the PBP1B–LpoB interface impaired PBP1B activation by LpoB in vivo and in vitro. LpoB versions that partially or completely lack the flexible N terminus could interact with and fully stimulate PBP1B in vitro, but were nonfunctional in the cell. This supports a model in which the OM-anchored LpoB has to reach through the PG mesh to interact with the UB2H domain of PBP1B and stimulate PG synthesis.

Results

LpoB Interacts with PBP1B and Stimulates both of Its Activities. To gain mechanistic and structural insights into the PBP1B–LpoB interaction, we purified both proteins and tested them in surface plasmon resonance (SPR) experiments. PBP1B was covalently bound to a chip surface with immobilized ampicillin. A soluble version of LpoB lacking the N-terminal lipid modification, LpoB(sol) (*SI Appendix*, Table S1), bound to immobilized PBP1B with rapid on/off rates, approaching binding saturation at a concentration of 4 μM, and with a K_d of 0.81 ± 0.08 μM (Fig. 1*A*). Binding of LpoB(sol) to a control surface without PBP1B was negligible (*SI Appendix*, Fig. S1*A*).

LpoB was previously shown to moderately enhance consumption of lipid II by PBP1B (1.5-fold) (3, 13) and to stimulate the TPase activity of PBP1B, yielding a highly peptide cross-linked PG (5, 13) (*SI Appendix*, Fig. S1*B*). As the effect of LpoB on the GTase activity of PBP1B does not require an active TPase, and reduces the average length of glycan strands (3), Lupoli et al. (13) proposed that the dominant effect of LpoB is on the GTase activity of PBP1B (*Discussion*). To more accurately monitor the rate of GTase activity, we used a continuous assay with a fluorescently labeled dansyl-lipid II as a substrate (7). In this assay, LpoB(sol) increased the maximal GTase rate of PBP1B 8-fold (Fig. 1*B*; see Fig. 4*C*). The noncognate LpoA, which specifically interacts with PBP1A, had no effect on the GTase activity of PBP1B. As expected, this activity was completely inhibited by the antibiotic moenomycin. Interestingly, LpoB significantly stimulated the GTase activity of PBP1B even at pH 4.5, at which PBP1B alone was virtually inactive (*SI Appendix*, Fig. S1*C*), suggesting that LpoB might induce conformational changes in the GTase domain to maintain the catalytic Glu233 residue in an active, unprotonated state even at this low pH.

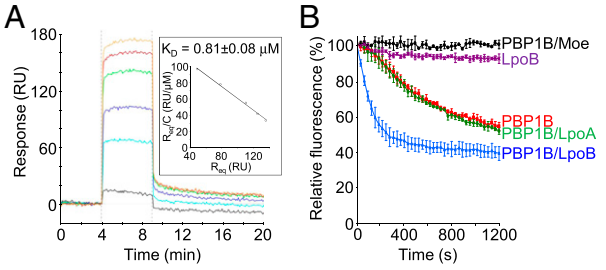

Fig. 1. LpoB interacts with PBP1B and enhances the rate of its GTase activity. (*A*) LpoB–PBP1B interaction dynamics measured by SPR. LpoB was injected at concentrations of 0 (black line), 0.5 (light blue), 1 (dark blue), 2 (green), 3 (red), and 4 (orange) μM to a chip surface with immobilized PBP1B (*SI Appendix*, Fig. S1*A* shows control). The response at equilibrium R_{eq}, normalized to the injected concentration C (R_{eq}/C), plotted against R_{eq}, yields a straight line with a slope of $-K_d^{-1}$ (*Inset*). The average K_d value ± SD was determined from three independent experiments. (*B*) Continuous GTase assay for PBP1B, measuring consumption of fluorescently labeled substrate (dansyl-lipid II). PBP1B activity (red) is stimulated by LpoB (blue) but not by LpoA (green). The antibiotic moenomycin (Moe) inhibits PBP1B GTase activity (black). LpoB alone (purple) shows no activity. Each measurement is shown as mean ± SD of three independent experiments.

Structure of LpoB. Purified LpoB(sol) eluted as a single peak in size-exclusion chromatography with a calculated molecular weight of 45.5 ± 3.3 kDa, which is more than double the theoretical value of 20.3 kDa (*SI Appendix*, Fig. S2*A*). However, this peak remained the same at a wide range of NaCl concentrations (0.1–2 M), arguing against LpoB multimerization. A single monomer peak with a sedimentation coefficient of 1.754 S (*SI Appendix*, Fig. S2*B*) could be seen in analytical ultracentrifugation, which is unusually high for a protein of this size, indicating that LpoB(sol) has an elongated molecular shape and/or extended flexible regions.

We opted to use NMR spectroscopy to determine the structure of LpoB(sol), as the presence of large disordered regions often prevents the crystallization of proteins. NMR data were recorded on a [^{13}C,^{15}N]LpoB(sol) sample and the backbone and side-chain ^{1}H,^{13}C,^{15}N-resonances were assigned by using conventional and targeted experiments to identify the residues in the proline-rich region in the N terminus (14). Automatically and manually assigned unambigous distance restraints (N = 3,849) and ϕ/ψ dihedral angles (N = 248) were derived from Nuclear Overhauser Effect (NOE) data and chemical shifts, respectively, and used for further structure calculation. LpoB(sol) has two structurally distinct parts, a disordered region near the N terminus (up to Pro73) and a well-folded globular domain (His74 to Gln213; Fig. 2*A*). The N terminus contains 27.7% Pro residues and is predicted as disordered by IUPred (15). The high structural flexibility from Val21 to Pro73 was confirmed by (*i*) medium- to long-range NOE correlations being absent, (*ii*) a negative {^{1}H}-^{15}N relaxation NOE value for Val21 to Ala69 amide resonances (Fig. 2*B*), and (*iii*) an inability to identify any secondary structure elements between Val21 and Pro73 when entering ^{1}H, ^{13}C, and ^{15}N-backbone chemical shifts into the δ2D software (16). This large disordered region has an estimated maximal length of ∼145 Å, which explains the high analytical ultracentrifugation sedimentation coefficient.

After refinement, the 20 lowest-energy high-resolution structures of LpoB(sol) were selected and the rmsd values to the average structure were calculated for the backbone (0.18 ± 0.03 Å) and heavy (0.44 ± 0.06 Å) atoms of the globular domain (His74 to Gln213; Fig. 2*A* and *SI Appendix*, Table S2). LpoB comprises a three-stranded antiparallel β-sheet (β2, 175–183; β3, 189–196; and β4, 200–209), which is flanked by a short two-stranded parallel β-sheet (β1, 102–105; β2, 175–178) and four α-helices (H1, 79–93; H2, 118–132; H3, 140–150; H4, 161–171). H3 and H4 are tightly linked with the parallel β-sheet by a hydrophobic core involving H3–β1, H4–β1, and H4–β2 contacts. H1 and H2 are stabilized at the antiparallel β-sheet through hydrophobic contacts between H1, H2, β2, and, in part, β4.

The globular domain of LpoB has a large positively charged patch on the three-stranded β-sheet with an extension toward α-helix H4, and a smaller positive patch between H1 and H2 on the other side of the molecule (*SI Appendix*, Fig. S3*A*). Interestingly, the large positive patch contains highly conserved residues in the three-stranded β-sheet (β2, 175–179; β3, 192–195; and β4, 200–206), as determined by aligning 68 distinct LpoB sequences (*SI Appendix*, Fig. S3 *B–D*). We reasoned that this

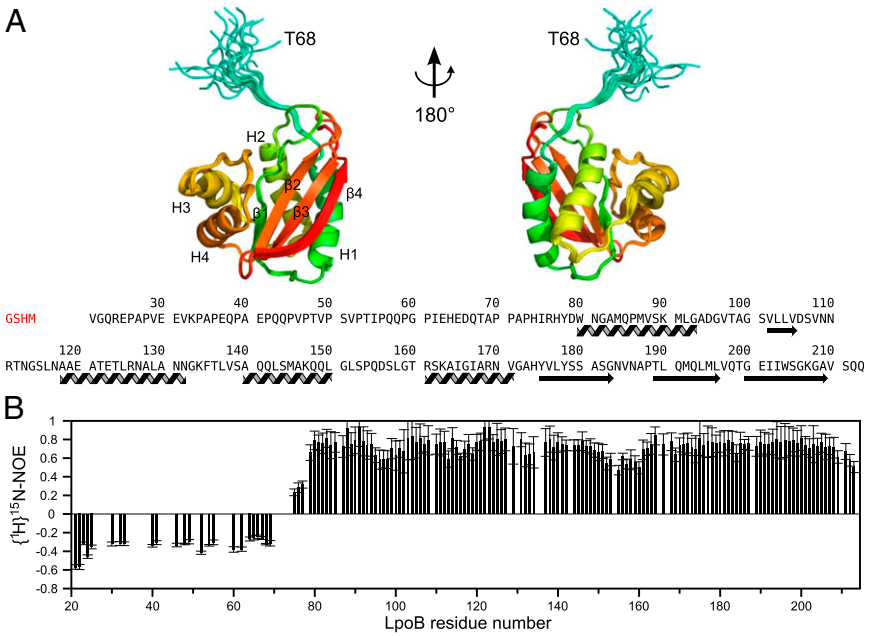

Fig. 2. LpoB structure shows a globular domain with a flexible N-terminal region. (*A*) Ensemble of the 20 lowest-energy structures of LpoB(sol) (from Thr68 for clarity) determined by NMR spectroscopy (colors from cyan to red are from N to C terminus). The position of α-helices (H1–H4) and β-strands (β1–β4) are indicated on the structure and on the sequence below (helices and arrows). (*B*) Heteronuclear $\{^1H\}$-^{15}N-NOE values calculated from the intensity ratio between the saturated and the reference experiments. Errors on the intensity ratio were calculated from the signal-to-noise ratio of the NMR signal in each spectrum. The numbering begins at Val21. High, low, and negative values indicate low, medium, and high flexibility, respectively.

conserved and rather concave surface could potentially serve as an interaction site with PBP1B.

LpoB–UB2H (PBP1B) Interaction. LpoB has coevolved with the small noncatalytic UB2H domain of PBP1B (5), which is situated between its GTase and TPase domains (12). LpoB can be chemically cross-linked to PBP1B in vivo, but not to a version that lacks UB2H (5). We purified an oligohistidine-tagged UB2H domain (His-UB2H) (12), which, as expected, bound to LpoB, but not LpoA (*SI Appendix*, Fig. S4*A*). To map more precisely the LpoB–PBP1B interaction site, spectra from an $[^1H,^{15}N]$-BEST-TROSY-HSQC experiment were recorded on $[^{13}C,^{15}N]$LpoB (sol) alone and with a 2-fold molar excess of unlabeled His-UB2H. Superimposition of the spectra revealed 45 perturbed LpoB amide resonances (*SI Appendix*, Fig. S4 *B* and *C*). When LpoB was progressively added to the LpoB–UB2H sample, changing the ratio of the two proteins, the LpoB resonances shifted closer to their original positions in the free LpoB spectrum. This suggests an intermediate-to-fast exchange regime between the two protein forms, which is fully consistent with a K_d in the micromolar range for LpoB(sol):PBP1B (Fig. 1*A*). Chemical shift and resonance intensity perturbations were mapped on the LpoB (sol) structure (Fig. 3*A*) and were found to concentrate on a conserved region, which included β2, β3, and the tip of H4 (*SI Appendix*, Fig. S3 *B–E*). Incorporating this information into the docking software HADDOCK (17), we could identify two possible interfaces in the UB2H domain of PBP1B, involving a common stretch (167–176) and two exclusive stretches (147–152 and 188–193; *SI Appendix, Supplemental Materials and Methods*). Further biochemical and phenotypic analysis (Fig. 4 and *SI Appendix*, Table S3) supported the latter interface, allowing us to refine the docking model. In the resulting most populated ensemble of LpoB–UB2H structures (Fig. 3*B*), the short β-turn (187–188)–β-strand (190–191) of UB2H stacks between β2 and H4 of LpoB(sol).

The LpoB–UB2H Interaction Is Required for the Function of PBP1B. We constructed a number of PBP1B and LpoB alleles carrying single Ala, multiple Ala, or charge-reversing substitutions in amino acids predicted to be part of the LpoB–UB2H interface, and tested them for binding and activity. PBP1B interface variants carrying single or double amino acid substitutions were only partially active in vivo (Fig. 4*A* and *SI Appendix*, Fig. S5*B*; cefsulodin targets mainly PBP1A, leaving cells dependent on PBP1B) and did not suffice for cell growth without PBP1A (*SI Appendix*, Table S3). PBP1B R190D lost nearly all in vivo activity, but we had to introduce multiple Ala substitutions in PBP1B for such a strong effect (Fig. 4*A* and *SI Appendix*, Fig. S5). These results were mirrored when we measured K_d values of the LpoB–PBP1B interaction (Fig. 4*B* and *SI Appendix*, Fig. S6) and in vitro GTase and

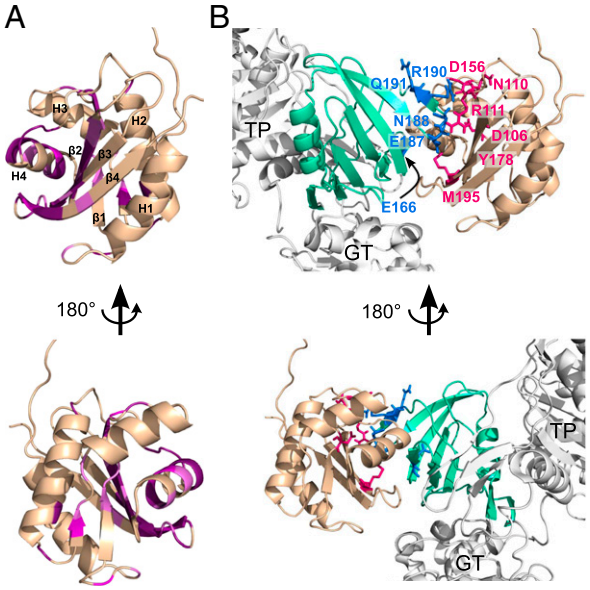

Fig. 3. LpoB interacts with the UB2H domain of PBP1B. (*A*) Residues showing a significant perturbation upon His-UB2H addition are mapped on the cartoon representation of the LpoB(sol) structure. Residues showing chemical shift perturbations higher than 0.05 ppm are shown in pink, and residues for which the $[^1H,^{15}N]$ correlation showed intensity changes upon interaction are in dark purple (*SI Appendix*, Fig. S4*C*). (*B*) Final HADDOCK model of the LpoB–PBP1B complex after addition of ambiguous restraints from NMR perturbations, and biochemical/functional data (Fig. 4). Residues changed to Ala, or reverse-charge amino acids in the activity assays, are represented as sticks in blue (UB2H domain) or magenta (LpoB). Cartoon representation of LpoB and UB2H domain are shown in wheat and green, respectively. Additional domains in PBP1B are shown in gray.

MICROBIOLOGY

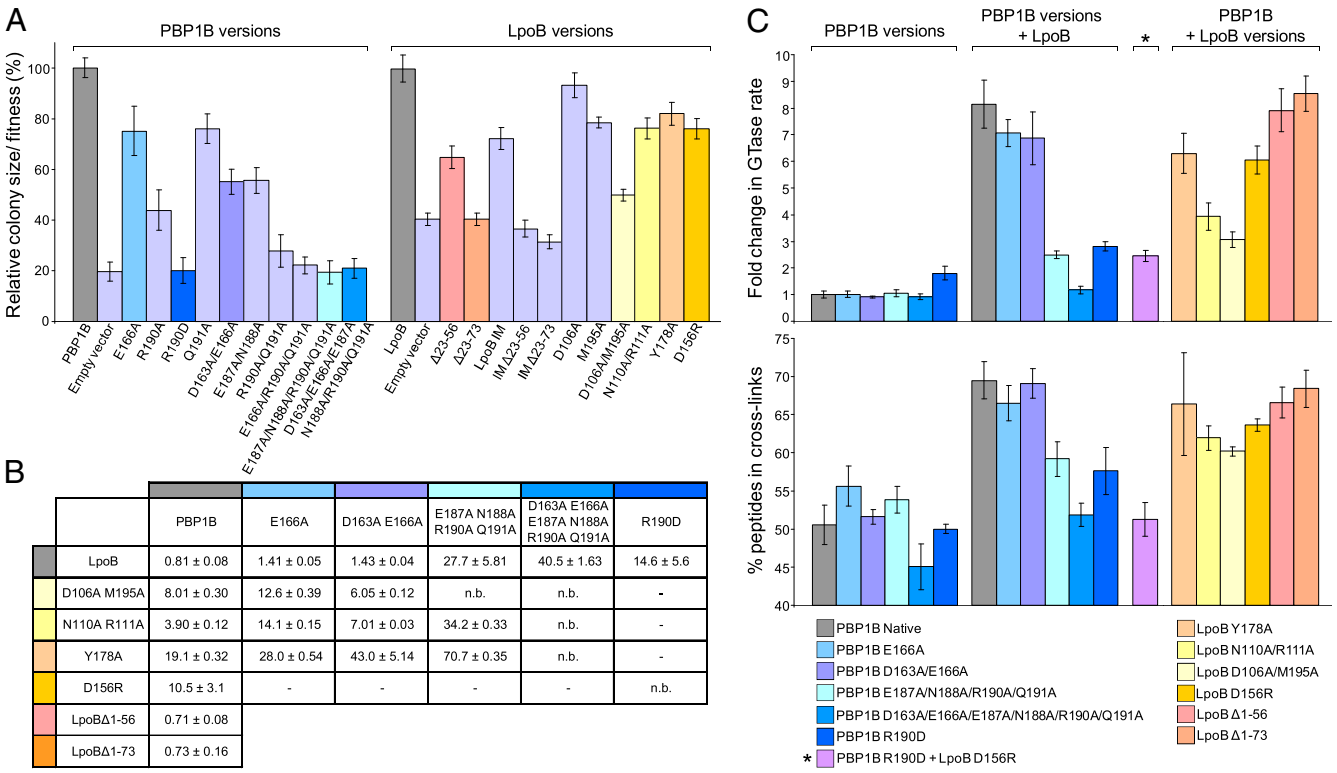

Fig. 4. Dissecting the LpoB–PBP1B interaction and its relevance for PBP1B function. (*A*) In vivo activity of PBP1B and LpoB versions as measured by cellular fitness under cefsulodin treatment (12 and 24 μg/mL for PBP1B and LpoB versions, respectively). Cefsulodin targets primarily PBP1A, increasing the cell's dependence on PBP1B. Colony size is used as proxy of cellular fitness, and the colony size relative to cells expressing the WT protein is plotted here (mean ± SD; $n > 12$). (*B*) K_d values in μM determined by SPR of the PBP1B–LpoB interaction by using different PBP1B and LpoB versions (mean ± SD, $n = 3$). n.b., insufficient binding for determination of K_d; -, not tested. (*C*) GTase or TPase activity assays for PBP1B using different PBP1B and LpoB versions. The GTase rate is compared with the mean rate of PBP1B alone (mean ± SD; $n = 3$–6). The TPase activity is shown as percentages of cross-linked peptides in PG (mean ± SD; $n = 3$–4).

TPase activities of some of the PBP1B mutant in the presence and absence of LpoB (Fig. 4*C* and *SI Appendix*, Figs. S7 and S8). PBP1B R190D and the quadruple PBP1B Ala mutant with a defected interface between 187 and 191 had ∼20- and 30-fold weaker interaction to LpoB, respectively (Fig. 4*B* and *SI Appendix*, Fig. S6), and could only be basally activated by LpoB in vitro, although they were as active as WT PBP1B when assayed without LpoB (Fig. 4*C* and *SI Appendix*, Figs. S7 and S8). A PBP1B version with two further substitutions (D163A and E166A) was completely insensitive to LpoB activation in vivo and in vitro (Fig. 4 and *SI Appendix*, Figs. S7 and S8).

LpoB versions with single, and especially double, Ala substitutions in D106, N110, R111, and M195, and a D156R charge reversal version, were less active in vivo (Fig. 4*A* and *SI Appendix*, Fig. S5*B*) and would not suffice for the cell to survive only with PBP1B (*SI Appendix*, Table S3; the substitutions did not affect the overall folding; *SI Appendix*, Fig. S9). In agreement with D106A and M195A having the strongest effect in vivo, this double mutant showed a strong increase in K_d (∼10-fold; Fig. 4*B* and *SI Appendix*, Fig. S6) and the most severe defect in stimulation of GTase rate and TPase activity (Fig. 4*C* and *SI Appendix*, Figs. S7 and S8). The combination of the charge-reversed versions PBP1B R190D and LpoB D156R did not yield a functional pair in the cell and in vitro (Fig. 4*C* and *SI Appendix*, Fig. S5*B*), although these residues lie within direct interaction proximity. This points to an important role of R190 in PBP1B in the stimulation mechanism. Interestingly, an Ala substitution in Y178, lying within β2 of LpoB, significantly decreased the interaction with PBP1B (∼25-fold; presumably by affecting the interface to amino acids 187–191 of PBP1B, as the quadruple PBP1B mutant showed a suppressive interaction with LpoB Y178A; Figs. 3*B* and 4*B* and *SI Appendix*, Fig. S6), but only moderately affected the in vivo or in vitro activation of PBP1B (Fig. 4 *A* and *C*). This suggests that binding is required but not sufficient for PBP1B activation by LpoB, and supports further a model in which LpoB activates PBP1B by inducing conformational changes in its catalytic domain(s).

Overall, these data indicate that PBP1B and LpoB interact through a large interface that involves several amino acids in both proteins, which is consistent with the NMR data and molecular docking simulations.

The N-Terminal Flexible Region of LpoB Is Vital for Its Function in Vivo. The NMR data preclude any secondary structure elements in the N-terminal region of LpoB, which suggests it could be a long flexible linker that anchors LpoB to the OM. We constructed LpoB versions with a truncated or absent N-terminal region (LpoBΔ1–56 and LpoBΔ1–73, respectively). Both interacted with PBP1B with a similar K_d as native LpoB (Fig. 4*B* and *SI Appendix*, Fig. S6), and were capable of fully stimulating its GTase and TPase activities in vitro (Fig. 4*C* and *SI Appendix*, Figs. S7 and S8), indicating that the flexible region is dispensable for activation of PBP1B in a purified-component assay. In contrast, the partial or complete lack of the flexible region rendered LpoB nonfunctional (i.e., no linker) or partially functional (i.e., truncated LpoB) in the cell (Fig. 4*A* and *SI Appendix*, Fig. S5 and Table S3). We have previously shown that full-length LpoB that is retained in the IM supports cell growth, even in the absence of LpoA–PBP1A (5). When retained in the IM, both LpoB versions with truncated or deleted N termini were nonfunctional (Fig. 4*A* and *SI Appendix*, Fig. S5). In toto, the long N-terminal linker is vital for LpoB in vivo, as it presumably allows it to reach PBP1B from afar (OM; *Discussion*). This region may have additional

roles, as it is still required in the IM-anchored LpoB, although UB2H now lies closer.

Discussion

Activation of PG Synthases from the OM. LpoA and LpoB are OM-anchored lipoproteins that share no homology to each other, and interact with discrete docking domains in their cognate PBP. Up to now, no structural information has been available on these activators and/or their interaction with the PG synthase. By using data from NMR spectroscopy and small-angle X-ray scattering, we have recently modeled the structure of LpoA, which has a rigid, elongated shape with a total length of 145 Å (18). The LpoB structure reported here is clearly distinct: a flexible N-terminal region as long as 145 Å, followed by a ∼30-Å-long globular domain. However, both proteins use different architectural features to achieve the same goal: to span more than two thirds of the 210-Å-wide periplasm (19) and reach their cognate IM-anchored PBP (Fig. 5 shows LpoB). The globular domain of LpoB and the rigid body of LpoA both have a diameter of ∼30 Å, allowing them to traverse the PG layer, which has ∼40–60-Å-wide pores depending on turgor (20, 21). As interlayer distances have been measured only for the lateral part of the *E. coli* envelope, length constraints and membrane separation could be different in the leading edge of the inward growing septum, where PBP1B–LpoB predominantly localizes and acts. This could explain why OM-anchored LpoB was still somewhat functional when the flexible region was significantly shortened by 34 aa (removal of residues 23–56), although not to a degree that would allow cells to survive only on PBP1B/LpoB. When in the IM, LpoB lies closer to UB2H, yet a truncation or removal of its flexible linker was not tolerated. This suggests that the N terminus of LpoB may not merely be a linker but may have additional roles, e.g., interaction with other proteins. Efforts to elucidate its function are under way.

PBP1B interacts with the essential, IM-anchored cell division proteins PBP3 and FtsN (8, 10). FtsN also stimulates the activity of PBP1B, presumably by stabilizing its dimeric form, which is more active in in vitro assays (22). FtsN has a long flexible stretch of ∼120 aa, which allows it to reach and bind to the PG via its C-terminal SPOR domain (23, 24). It is interesting that both proteins stimulating PBP1B, LpoB and FtsN, share long flexible stretches, albeit anchored to different membranes. Such structural flexibility may be vital for dynamic multiprotein envelope complexes and may provide access for controlling the complex activity even from afar.

Globular Domain of LpoB Has Structural Similarity to TolB. The Dali server (25) identifies several structural homologs for the globular domain of LpoB. The top hits are a lipoprotein of unknown function, GNA1162 from *Neisseria meningitidis* [Protein Data Bank (PDB) ID code 4HRV (26); Z = 7.4, rmsd = 2.2 Å], and the N-terminal domain of *E. coli* TolB [TolB_N; PDB ID code 1CRZ (27); Z = 6.2, rmsd = 2.9 Å; *SI Appendix*, Fig. S10]. Interestingly, LpoB has the inverse orientation from TolB_N, with α-helix H1 of LpoB corresponding to the last α-helix of TolB_N. As a member of the Tol–Pal system, TolB participates in OM constriction during cell division, and the first 12 residues of its N-terminal domain interact with the IM protein TolA (28); LpoB lacks this TolA-binding motif. We have previously reported that PBP1B–LpoB and Tol–Pal complexes interact genetically and colocalize at constriction sites, implying that the two systems may have overlapping and/or interlinked functions during cell division (5). The structural similarity between LpoB and TolB_N points further toward a connection between the two machineries. TolB_N domains are found in most proteobacteria and chlamydiae, with many species carrying multiple periplasmic proteins with this domain, often in a Tol–Pal unrelated-genomic context. Interestingly, GNA1162 is part of the DUF799 family, which shows strong genomic co-occurrence and neighborhood with a TolB_N-containing protein (STRING). It is tempting to speculate that the two structurally related domains, TolB_N and DUF799, may work in concert in multiple contexts in the bacterial cell envelope.

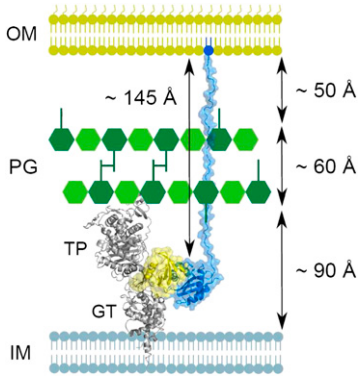

Fig. 5. Model of the stimulation of PBP1B by LpoB in the bacterial envelope. LpoB (blue) uses its ∼145-Å-long, flexible N-terminal region to span the periplasm and places its globular domain in position to interact with the UB2H domain of PBP1B (yellow). The thickness of the PG layer and distances to the IM and OM are according to previous studies (19).

How Does LpoB Activate PBP1B? We have identified amino acid residues in LpoB and the UB2H domain of PBP1B that are important for the PBP1B–LpoB interaction and the in vitro and in vivo function of PBP1B. In both proteins, often more than one amino acid had to be replaced by Ala to observe a measureable effect, and several amino acids had to be targeted to completely break the PBP1B–LpoB interaction. This is consistent with the NMR results, and points to an extended interface between the two proteins. Interestingly, in all PBP1B and LpoB versions with perturbed interface and/or activation, the GTase and TPase activities were affected in similar ways. This suggests that the two activities are interdependent, which is consistent with previous data (5, 13, 22). It may also mean that LpoB primarily activates one of the two PBP1B activities, and the second is affected as a result of the interlinking. As LpoB is capable of stimulating the GTase activity of PBP1B even at pH 4.5, it is likely that LpoB induces conformational changes in PBP1B that impact the environment of the catalytic Glu233 residue within the GTase domain. Such long-range allosteric effects on PBP activity are not without precedent. Recently, the binding of the antibiotic ceftaroline or PG fragments to an allosteric site was shown to open the catalytic TPase site of PBP2a from a methicillin-resistant *Staphylococcus aureus* strain over a distance of ∼60 Å (29). Further experiments are required to determine exactly how LpoB stimulates PBP1B. In any case, the quick on/off rates measured by SPR for the PBP1B–LpoB interaction suggest a highly dynamic interaction. This could be necessary for proper regulation of PBP1B by LpoB within a dynamic divisome.

Materials and Methods

Chemicals and Proteins. [^{14}C]GlcNAc-labeled and dansylated lipid II were prepared as published (22). [^{15}N]NH_4Cl and [^{13}C]glucose were purchased from Cambridge Isotope Labs. All other chemicals were from Sigma. The following proteins were prepared as previously described: PBP1B and versions of it with amino acid exchanges (8) and oligohistidine-tagged soluble LpoA [His-LpoA(sol)] (5). Soluble versions of LpoB with or without the oligohistidine-tag [His-LpoB(sol) and LpoB(sol)] and a His-tagged version of the UB2H domain of PBP1B (His-UB2H) were prepared as described in *SI Appendix, Supplemental Materials and Methods*. Antisera against PBP1B and LpoB (Eurogentec) were purified over an antigen column as described previously (8). VIM-4 β-lactamase was a gift from Adeline Derouaux (Centre for Bacterial Cell Biology, Newcastle University, Newcastle upon Tyne, United Kingdom). Cellosyl was provided by Hoechst.

Bacterial Strains and Growth Conditions. *E. coli* strains and plasmids used in this work are listed in *SI Appendix*, Table S1. For in vivo assays, cells were

MICROBIOLOGY

grown aerobically at 37 °C in Luria Bertani (LB) Lennox, and, where appropriate, antibiotics/inducers were added: ampicillin (100 μg/mL), kanamycin (30 μg/mL), chloramphenicol (20 μg/mL), and arabinose (10 mM). For protein purification, cells with the appropriate plasmids were grown in LB or M9 minimal medium with 0.3% glucose, pH 6.8–7.2. For ^{15}N uniformly labeled or $^{15}N/^{13}C$ uniformly NMR samples, cells were grown with M9 medium containing [^{15}N]NH_4Cl or [^{15}N]NH_4Cl and [^{13}C]glucose, respectively.

Complementation Experiments for PBP1B and LpoB Versions. All PBP1B versions tested were expressed from the pET28a vector at levels similar or slightly higher than that of the endogenous PBP1B; the only exception was the version with six point mutations, which was less stable in vivo and expressed at significantly lower levels than the endogenous PBP1B. LpoB versions were expressed from the pBAD30 vector, and induction was required to reach endogenous LpoB levels. All LpoB versions were at levels similar or higher than that of the endogenous LpoB and were correctly folded (*SI Appendix*, Fig. S9). Δ*mrcB* and Δ*lpoB* cells, carrying the different PBP1B and LpoB versions, were robotically arrayed on agar plates in a 384-array format, with each variant being present 24 times. Plates were replicate-pinned on new agar plates containing the stress (cefsulodin or A22) and 10 mM arabinose (LpoB variants), incubated overnight, and imaged. Colony sizes were assessed with in-house software.

Protein Interaction and Activity Assays. SPR experiments were performed with slight modifications to a previously described protocol (30), as described in *SI Appendix, Supplemental Materials and Methods*. Continuous fluorescence GTase assays were performed as described previously (7). Radiolabeled lipid II was used as described before to measure TPase activity in an in vitro PG synthesis assay (22).

NMR Spectroscopy. All NMR spectra were collected on Agilent spectrometers operating at 600 or 800 MHz ^1H NMR frequencies, except for an aliphatic ^{13}C-NOESY-HSQC experiment, which was recorded on a 950-MHz Bruker US spectrometer. All spectrometers were equipped with cryogenic triple-resonance probes. Steady-state {^1H}-^{15}N-NOE experiments with a 3-s proton presaturation period were collected at 600-MHz proton frequency (31). For structure determination, NMR spectra were recorded on a 0.8-mM [^{13}C,^{15}N]LpoB(sol) sample in 100 mM sodium acetate, pH 5.0, containing 10% (vol/vol) D_2O at 308 K (14). A 3D ^{15}N-NOESY-HSQC (150 ms mixing time) and 3D aliphatic, aromatic, and methyl-^{13}C-NOESY-HSQC (32) experiments (mixing times of 120, 130, and 160 ms) were used to access experimental structural information. Distance restraints were extracted and analyzed by using UNIO'10 as described in *SI Appendix, Supplemental Materials and Methods*. Interaction studies were performed at pH 7.5 and 298 K on a mixture of 150 μM [^{15}N,^{13}C]LpoB(sol) and 300 μM His-UB2H in a buffer containing 10 mM Tris·HCl, 10 mM $MgCl_2$, 100 mM NaCl, and 10% (vol/vol) D_2O. Models of LpoB docked onto the UB2H domain of PBP1B were built with the HADDOCK Web server for data-driven biomolecular docking of HADDOCK2.1 (17) as described in *SI Appendix, Supplemental Materials and Methods*.

ACKNOWLEDGMENTS. We thank Natalie Strynadka for communicating unpublished results and Che Ma for plasmid pET15bUB2H. This work was supported by Biotechnology and Biological Sciences Research Council BB/I020012/1 and European Commission DIVINOCELL HEALTH-F3-2009-223431 (to W.V.); French Infrastructure for Integrated Structural Biology ANR-10-INSB-05-02, Grenoble Alliance for Integrated Structural Biology ANR-10-LABX-49-01, and Très Grande Infrastructure de Recherche–Résonance Magnétique Nucléaire–Très Haut Champ (TGIR-RMN-THC) FR3050 from the Centre National de la Recherche Scientifique (CNRS) (to J.-P.S.); the Sofja Kovalevskaja award (to A.T.); and European Molecular Biology Laboratory (EMBL) funding (A.K.). N.L.J. holds a PhD fellowship (Contrat de Formation par la Recherche) from the Commissariat à l'Energie Atomique et aux Energies Alternatives. Part of this work was conducted by using the platforms of the Grenoble Instruct center (Integrated Structural Biology; Unité Mixte de service 3518, funded by CNRS, Commissariat à l'Energie Atomique, Université Joseph Fourier, and EMBL).

1. Vollmer W, Blanot D, de Pedro MA (2008) Peptidoglycan structure and architecture. *FEMS Microbiol Rev* 32(2):149–167.
2. Typas A, Banzhaf M, Gross CA, Vollmer W (2012) From the regulation of peptidoglycan synthesis to bacterial growth and morphology. *Nat Rev Microbiol* 10(2):123–136.
3. Paradis-Bleau C, et al. (2010) Lipoprotein cofactors located in the outer membrane activate bacterial cell wall polymerases. *Cell* 143(7):1110–1120.
4. Sham LT, Barendt SM, Kopecky KE, Winkler ME (2011) Essential PcsB putative peptidoglycan hydrolase interacts with the essential FtsXSpn cell division protein in *Streptococcus pneumoniae* D39. *Proc Natl Acad Sci USA* 108(45):E1061–E1069.
5. Typas A, et al. (2010) Regulation of peptidoglycan synthesis by outer-membrane proteins. *Cell* 143(7):1097–1109.
6. Yang DC, et al. (2011) An ATP-binding cassette transporter-like complex governs cell-wall hydrolysis at the bacterial cytokinetic ring. *Proc Natl Acad Sci USA* 108(45):E1052–E1060.
7. Banzhaf M, et al. (2012) Cooperativity of peptidoglycan synthases active in bacterial cell elongation. *Mol Microbiol* 85(1):179–194.
8. Bertsche U, et al. (2006) Interaction between two murein (peptidoglycan) synthases, PBP3 and PBP1B, in *Escherichia coli*. *Mol Microbiol* 61(3):675–690.
9. Fraipont C, et al. (2011) The integral membrane FtsW protein and peptidoglycan synthase PBP3 form a subcomplex in *Escherichia coli*. *Microbiology* 157(pt 1):251–259.
10. Müller P, et al. (2007) The essential cell division protein FtsN interacts with the murein (peptidoglycan) synthase PBP1B in *Escherichia coli*. *J Biol Chem* 282(50):36394–36402.
11. Egan AJF, Vollmer W (2013) The physiology of bacterial cell division. *Ann N Y Acad Sci* 1277:8–28.
12. Sung MT, et al. (2009) Crystal structure of the membrane-bound bifunctional transglycosylase PBP1b from *Escherichia coli*. *Proc Natl Acad Sci USA* 106(22):8824–8829.
13. Lupoli TJ, et al. (2014) Lipoprotein activators stimulate *Escherichia coli* penicillin-binding proteins by different mechanisms. *J Am Chem Soc* 136(1):52–55.
14. Jean NL, Bougault CM, Egan AJF, Vollmer W, Simorre JP (2014) Solution NMR assignment of LpoB, an outer-membrane anchored Penicillin-Binding Protein activator from *Escherichia coli*. *Biomol NMR Assign*, 10.1007/s12104-014-9557-z.
15. Dosztányi Z, Csizmok V, Tompa P, Simon I (2005) IUPred: Web server for the prediction of intrinsically unstructured regions of proteins based on estimated energy content. *Bioinformatics* 21(16):3433–3434.
16. Camilloni C, De Simone A, Vranken WF, Vendruscolo M (2012) Determination of secondary structure populations in disordered states of proteins using nuclear magnetic resonance chemical shifts. *Biochemistry* 51(11):2224–2231.
17. de Vries SJ, van Dijk M, Bonvin AM (2010) The HADDOCK web server for data-driven biomolecular docking. *Nat Protoc* 5(5):883–897.
18. Jean NL, et al. (2014) The elongated molecular structure of the outer-membrane activator of peptidoglycan synthesis LpoA: Implications for PBP1A-stimulation. *Structure*, in press.
19. Matias VR, Al-Amoudi A, Dubochet J, Beveridge TJ (2003) Cryo-transmission electron microscopy of frozen-hydrated sections of *Escherichia coli* and *Pseudomonas aeruginosa*. *J Bacteriol* 185(20):6112–6118.
20. Demchick P, Koch AL (1996) The permeability of the wall fabric of *Escherichia coli* and *Bacillus subtilis*. *J Bacteriol* 178(3):768–773.
21. Vázquez-Laslop N, Lee H, Hu R, Neyfakh AA (2001) Molecular sieve mechanism of selective release of cytoplasmic proteins by osmotically shocked *Escherichia coli*. *J Bacteriol* 183(8):2399–2404.
22. Bertsche U, Breukink E, Kast T, Vollmer W (2005) *In vitro* murein peptidoglycan synthesis by dimers of the bifunctional transglycosylase-transpeptidase PBP1B from *Escherichia coli*. *J BiolChem* 280(45):38096–38101.
23. Ursinus A, et al. (2004) Murein (peptidoglycan) binding property of the essential cell division protein FtsN from *Escherichia coli*. *J Bacteriol* 186(20):6728–6737.
24. Yang JC, Van Den Ent F, Neuhaus D, Brevier J, Löwe J (2004) Solution structure and domain architecture of the divisome protein FtsN. *Mol Microbiol* 52(3):651–660.
25. Holm L, Rosenström P (2010) Dali server: Conservation mapping in 3D. *Nucleic Acids Res* 38(Web server issue):W545-9.
26. Cai X, et al. (2013) Structure of *Neisseria meningitidis* lipoprotein GNA1162. *Acta Crystallogr Sect F Struct Biol Cryst Commun* 69(pt 4):362–368.
27. Abergel C, et al. (1999) Structure of the *Escherichia coli* TolB protein determined by MAD methods at 1.95 Å resolution. *Structure* 7(10):1291–1300.
28. Bonsor DA, et al. (2009) Allosteric beta-propeller signalling in TolB and its manipulation by translocating colicins. *EMBO J* 28(18):2846–2857.
29. Otero LH, et al. (2013) How allosteric control of *Staphylococcus aureus* penicillin binding protein 2a enables methicillin resistance and physiological function. *Proc Natl Acad Sci USA* 110(42):16808–16813.
30. Vollmer W, von Rechenberg M, Höltje J-V (1999) Demonstration of molecular interactions between the murein polymerase PBP1B, the lytic transglycosylase MltA, and the scaffolding protein MipA of *Escherichia coli*. *J BiolChem* 274(10):6726–6734.
31. Farrow NA, et al. (1994) Backbone dynamics of a free and phosphopeptide-complexed Src homology 2 domain studied by ^{15}N NMR relaxation. *Biochemistry* 33(19):5984–6003.
32. Van Melckebeke H, Simorre JP, Brutscher B (2004) Suppression of artifacts induced by homonuclear decoupling in amino-acid-type edited methyl ^1H-^{13}C correlation experiments. *J Magn Reson* 170(2):199–205.